**ETH-Bibliothek Zürich, E-Periodica, https://www.e-periodica.ch**

# Approximate Analysis of the Stability of Single-Cell Folded Plate Structures

*Analyse approximative de la stabilité des structures en voiles prismatiques unicellulaires*

*Stabilitäts-Näherungsberechnung einzelliger Faltwerke*

S. E. SWARTZ

Assistant Professor of Civil Engineering, Kansas State University, Manhattan, Kansas, Formerly, Post Doctoral Research Associate, Illinois Institute of Technology, Chicago

S. A. GURALNICK

Professor of Civil Engineering, Illinois Institute of Technology, Chicago

## Introduction

Several procedures for the analysis of folded plate structures have been developed [7, 8, 9, 16, 22, 23, 25] for the determination of stresses throughout such structures. Many folded plate roofs have been built based on these analyses and have apparently performed quite satisfactorily. Some experimental studies [2, 8, 15] have also been performed and, in general, indicate results for stresses which agree satisfactorily with those obtained from theoretical analyses. To the writers' knowledge however, no analysis has been presented previously to indicate the possibility of buckling in a folded plate structure. A possibility exists that some sort of buckling could take place under the action of live loads smaller in magnitude than the service loads obtained by conventional techniques, especially for structures with large length to depth ratios. Such buckling as may occur could be either a general instability of the entire structure accompanied by a distortion of the cross-section (analogous to lateral instability of long beams), or a local buckling of the individual plate elements. This paper is concerned solely with the latter problem. Only single span, single-cell, simply supported structures subjected to uniform load on the horizontal projection are considered herein.

## General Description of the Local Buckling Problem

An individual plate element of a folded plate structure may be considered to be elastically supported along its longitudinal edges and simply supported along its transverse edges. Such a plate is subjected to uniform normal and tangential loads which give rise, through the structural action of the folded plate system, to internal normal shears and moments, and to in-plane forces, shears and moments. Following BLEICH [3], the buckling may be considered to be caused essentially by the in-plane forces. To correctly perform the analysis, all of these in-plane forces should be taken into account at the same time. In order to simplify this extremely complex problem, the local plate buckling is assumed to be caused primarily by either transverse in-plane forces or by the combined action of shearing and longitudinal in-plane forces. The first case is denoted "Transverse Buckling" and may be expected to occur for relatively low values of the span to depth ratio of the structure. The second case is denoted "Shear-Longitudinal Buckling" and may be expected to occur for relatively large values of the span to depth ratio. Such an analysis is an approximation at best and should be thought of as merely a first step in a general treatment of this problem. It is hoped that the analysis presented herein will provide sufficient insight into the problem to indicate possible directions for further refinement.

## Transverse Buckling Analysis

The procedure used herein to determine the load corresponding to transverse buckling in an individual plate element of a folded plate structure is based upon Rayleigh's Principle [20] and it utilizes a deflection field which merely satisfies the boundary conditions for an individual plate. To find such a deflection field, a general folded plate analysis may be used. Of the many folded plate analyses available only a few [9, 22] are sufficiently general to be applicable to a buckling analysis. The one used in this study is the method of GOLDBERG and LEVE [9]. The following assumptions are implicit in this method:

1. The structural system is assumed to act as a combination of slabs on elastic foundations at the ridges for "out of plane" deflections and as plates or beams for "in plane" deflections.
2. The plate elements are assumed to be supported on end diaphragms which are perfectly rigid parallel to the plane of the diaphragm and are perfectly flexible normal to the plane of the diaphragm.
3. The thickness of each plate is small compared to its other dimensions.
4. Small deflections are assumed throughout.
5. The material is assumed to be perfectly homogeneous, isotropic, and elastic.

With these assumptions an "elasticity solution" is obtained which relates the internal forces and deformations to the applied loads.

Fig. 1 shows a typical plate element together with an $x$, $y$, $z$ coordinate system. Positive orientation for the internal forces and deformations are also shown in this figure. The loads, forces, and deformations are expressed as
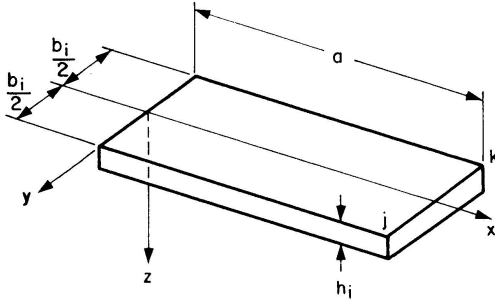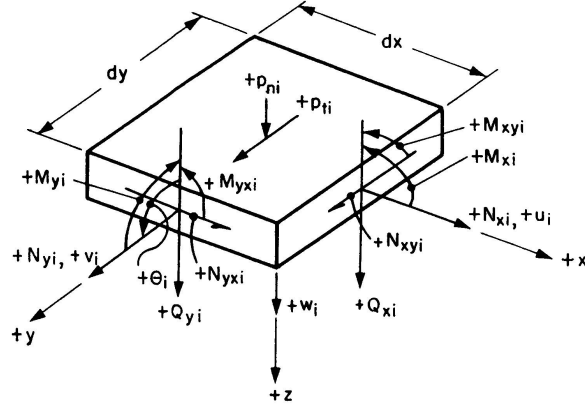
Fig. 1a. Coordinate system for
typical ($i$th) plate.

Fig. 1b. Plate element and associated forces
and displacements.

trigonometric series in the $x$-direction. For the $i$th plate, the relationships for the pertinent internal forces and deformations for a mode $m$ of the trigonometric series are [26]:

$$M_{y_i} = M_{Fy_i} + D_{1i} \frac{m\pi}{a} \sin \frac{m\pi x}{a} \left[ \left( A_{1i} \frac{m\pi y}{a} + A_{2i} \right) \sinh \frac{m\pi y}{a} \right.$$

$$\left. + \left( A_{3i} \frac{m\pi y}{a} + A_{4i} \right) \cosh \frac{m\pi y}{a} \right] ; \tag{1a}$$

$$N_{y_i} = N_{Fy_i} + D_{2i} \frac{m\pi}{a} \sin \frac{m\pi x}{a} \left[ \left( A_{5i} \frac{m\pi y}{a} + A_{6i} \right) \sinh \frac{m\pi y}{a} \right.$$

$$\left. + \left( A_{7i} \frac{m\pi y}{a} + A_{8i} \right) \cosh \frac{m\pi y}{a} \right] ; \tag{1b}$$

$$N_{x_i} = N_{Fx_i} + D_{2i} \frac{m\pi}{a} \sin \frac{m\pi x}{a} \left[ \left( A_{9i} \frac{m\pi y}{a} + A_{10i} \right) \sinh \frac{m\pi y}{a} \right.$$

$$\left. + \left( A_{11i} \frac{m\pi y}{a} + A_{12i} \right) \cosh \frac{m\pi y}{a} \right] ; \tag{1c}$$

$$N_{xy_i} = N_{Fxy_i} + D_{2i} \frac{m\pi}{a} \cos \frac{m\pi x}{a} \left[ \left( A_{13i} \frac{m\pi y}{a} + A_{14i} \right) \sinh \frac{m\pi y}{a} \right.$$

$$\left. + \left( A_{15i} \frac{m\pi y}{a} + A_{16i} \right) \cosh \frac{m\pi y}{a} \right] ; \tag{1d}$$

$$w_i \quad = \frac{1}{2}\sin\frac{m\,\pi\,x}{a}\left[(-A_{1i}\,y+A_{17i})\sinh\frac{m\,\pi\,y}{a}\right.$$

$$\left.+(-A_{3i}\,y+A_{18i})\cosh\frac{m\,\pi\,y}{a}\right]; \tag{1e}$$

$$\theta_i \quad = \frac{1}{2}\left[\left(-A_{1i}-A_{3i}\frac{m\,\pi\,y}{a}+\frac{m\,\pi}{a}A_{18i}-\frac{8\,a^3\,p_{ni}\lambda_{3m}\,k_{cm}}{m^4\,\pi^4\,D_i}\right)\sinh\frac{m\,\pi\,y}{a}\right. \tag{1f}$$

$$\left.+\left(-A_{1i}\frac{m\,\pi\,y}{a}+\frac{m\,\pi}{a}A_{17i}-A_{3i}+\frac{8\,a^2\,p_{ni}\lambda_{3m}\,y}{m^3\,\pi^3\,D_i}\right)\cosh\frac{m\,\pi\,y}{a}\right]\sin\frac{m\,\pi\,x}{a}.$$

In the above $M_{Fy_i}$, $N_{Fy_i}$, $N_{Fx_i}$, $N_{Fxy_i}$ are the internal forces induced by the applied loads and the condition of fixity at the edges and may be expressed for mode $m$ as follows [9]:

$$M_{Fy_i} \quad = -\frac{4\,a^2\,p_{ni}\,(1-\nu_i)}{m^3\,\pi^3}\sin\frac{m\,\pi\,x}{a}\left[-\frac{\nu_i}{1-\nu_i}\right.$$

$$\left.+\frac{\dfrac{m\,\pi\,y}{a}\sinh\dfrac{m\,\pi\,y}{a}+\left(\dfrac{1+\nu_i}{1-\nu_i}-\alpha_m\coth\alpha_m\right)\cosh\dfrac{m\,\pi\,y}{a}}{\alpha_m\operatorname{csch}\alpha_m+\cosh\alpha_m}\right]; \tag{2a}$$

$$N_{Fy_i} \quad = \frac{8\,a\,p_{ti}}{m^2\,\pi^2\left(\alpha_m\operatorname{csch}\alpha_m+\dfrac{3-\nu_i}{1+\nu_i}\cosh\alpha_m\right)}\sin\frac{m\,\pi\,x}{a}\left[-\left(\frac{2}{1+\nu_i}\right.\right.$$

$$\left.\left.+\alpha_m\coth\alpha_m\right)\sinh\frac{m\,\pi\,y}{a}+\frac{m\,\pi\,y}{a}\cosh\frac{m\,\pi\,y}{a}\right]; \tag{2b}$$

$$N_{Fx_i} \quad = -\frac{8\,a\,p_{ti}}{m^2\,\pi^2\left(\alpha_m\operatorname{csch}\alpha_m+\dfrac{3-\nu_i}{1+\nu_i}\cosh\alpha_m\right)}\sin\frac{m\,\pi\,x}{a}\left[-\left(k_{cm}-\frac{2\,\nu_i}{1+\nu_i}\right)\right.$$

$$\left.\cdot\sinh\frac{m\,\pi\,y}{a}+\frac{m\,\pi\,y}{a}\cosh\frac{m\,\pi\,y}{a}\right]; \tag{2c}$$

$$N_{Fxy_i} \quad = \frac{4\,a\,p_{ti}}{m^2\,\pi^2}\cos\frac{m\,\pi\,x}{a}\left\{2\left(\alpha_m\operatorname{csch}\alpha_m+\frac{3-\nu_i}{1+\nu_i}\cosh\alpha_m\right)^{-1}\right.$$

$$\left.\cdot\left[\frac{m\,\pi\,y}{a}\sinh\frac{m\,\pi\,y}{a}-\left(\alpha_m\coth\alpha_m+\frac{1-\nu_i}{1+\nu_i}\right)\cosh\frac{m\,\pi\,y}{a}\right]+1\right\}. \tag{2d}$$

In Eqs. (1) the terms $A_{1i}$ through $A_{18i}$ reflect the influence of the ridge deformations for mode $m$ on the internal forces and deformations in the $i$th plate. These terms are:

$$A_{1i} \quad = -\lambda_{1m}\,(\bar{\theta}_j+\bar{\theta}_k)+\lambda_{3m}\frac{m\,\pi}{a}\,(\bar{w}_{jk}+\bar{w}_{kj}).$$

$$A_{2i} \quad = \lambda_{2m}\,(\mu_{1i}-k_{cm})\,(\bar{\theta}_j+\bar{\theta}_k)+\lambda_{4m}\frac{m\,\pi}{a}\,(\mu_{3i}-k_{tm})\,(-\bar{w}_{jk}+\bar{w}_{kj}).$$

$$A_{3i} \quad = +\lambda_{2m}\,(\bar{\theta}_j+\bar{\theta}_k)-\lambda_{4m}\frac{m\,\pi}{a}\,(\bar{w}_{jk}-\bar{w}_{kj}).$$

$$A_{4i} = \lambda_{1m}(\mu_{1i} - k_{tm})(-\bar{\theta}_j + \bar{\theta}_k) + \frac{m\pi}{a}\lambda_{3m}(\mu_{3i} - k_{cm})(\bar{w}_{jk} + \bar{w}_{kj}).$$

$$A_{5i} = \lambda_{5m}(\bar{v}_{jk} - \bar{v}_{kj}) - \lambda_{7m}(\bar{u}_j + \bar{u}_k).$$

$$A_{6i} = \lambda_{6m}(\mu_{5i} + k_{cm})(\bar{v}_{jk} + \bar{v}_{kj}) + \lambda_{8m}(\mu_{6i} - k_{tm})(\bar{u}_j - \bar{u}_k).$$

$$A_{7i} = -\lambda_{6m}(\bar{v}_{jk} + \bar{v}_{kj}) + \lambda_{8m}(\bar{u}_j - \bar{u}_k).$$

$$A_{8i} = \lambda_{5m}(\mu_{5i} + k_{tm})(-\bar{v}_{jk} + \bar{v}_{kj}) - \lambda_{7m}(\mu_{6i} - k_{cm})(\bar{u}_j + \bar{u}_k).$$

$$A_{9i} = -A_{5i}.$$

$$A_{10i} = \lambda_{6m}(\mu_{4i} - k_{cm})(\bar{v}_{jk} + \bar{v}_{kj}) + \lambda_{8m}(\mu_{7i} - k_{tm})(-\bar{u}_j + \bar{u}_k).$$

$$A_{11i} = -A_{7i}.$$

$$A_{12i} = \lambda_{5m}(\mu_{4i} - k_{tm})(-\bar{v}_{jk} + \bar{v}_{kj}) + \lambda_{7m}(\mu_{7i} - k_{cm})(\bar{u}_j + \bar{u}_k).$$

$$A_{13i} = A_{7i}.$$

$$A_{14i} = \lambda_{5m}(\mu_{6i} + k_{tm})(-\bar{v}_{jk} + \bar{v}_{kj}) - \lambda_{7m}(\mu_{5i} - k_{cm})(\bar{u}_j + \bar{u}_k).$$

$$A_{15i} = A_{5i}.$$

$$A_{16i} = \lambda_{6m}(\mu_{6i} + k_{cm})(+\bar{v}_{jk} + \bar{v}_{kj}) + \lambda_{8m}(\mu_{5i} - k_{tm})(\bar{u}_j - \bar{u}_k).$$

$$A_{17i} = \frac{a}{m\pi}k_{cm}\lambda_{2m}(\bar{\theta}_j + \bar{\theta}_k) + (1 + k_{tm})\lambda_{4m}(-\bar{w}_{jk} + \bar{w}_{kj}).$$

$$A_{18i} = \frac{a}{m\pi}\lambda_{1m}k_{tm}(-\bar{\theta}_j + \bar{\theta}_k) + (1 + k_{cm})\lambda_{3m}(\bar{w}_{jk} + \bar{w}_{kj}).$$

In the above, $\bar{\theta}_j$, $\bar{w}_{jk}$, $\bar{v}_{jk}$, $\bar{u}_j$, and $\bar{\theta}_k$, $\bar{w}_{kj}$, $\bar{v}_{kj}$, $\bar{u}_k$ are the maximum values for a given mode $m$ of the rotation, normal, transverse and longitudinal displacements at edges $j$ and $k$ respectively of the $i$th plate. The plate coefficients $D_i$, $D_{1i}$, $D_{2i}$, $\lambda_{1m}$, $\lambda_{2m}$, $\lambda_{3m}$, $\lambda_{4m}$, $\lambda_{5m}$, $\lambda_{6m}$, $\lambda_{7m}$, $\lambda_{8m}$, $\alpha_m$, $k_{cm}$, $k_{tm}$, $\nu_i$, $\mu_{1i}$, $\mu_{3i}$, $\mu_{4i}$, $\mu_{5i}$, $\mu_{6i}$, $\mu_{7i}$ are defined in the Appendix.

$w_i$ is a solution of the homogeneous plate equation which satisfies the boundary conditions at the edges of the plate. In addition to the above, expressions can also be determined for $M_{x_i}$, $M_{xy_i}$, $Q_{x_i}$ and $Q_{y_i}$.

Using the deflection field, $w_i$, the total strain energy of bending, $U_{Ti}$, for a load on the $i$th plate is calculated along with the total external energy of the transverse loads, $T_{Ti}$. The change in strain energy from the previous value as the load is increased by a specified increment is $U_i$. The corresponding change in the external energy is $T_i$. The total external energy associated with the normal load is $\psi_{Ti}$ and the energy change as the load is increased by a specified increment is $\psi_i$. The change in kinetic energy associated with the increase in load is $V_i$.

Following the principle of the conservation of energy [20],

$$\psi_i + T_i = U_i + V_i. \tag{3}$$

If $U_i - T_i \leqq 0$ all energy associated with the normal load is converted into kinetic energy. The requirement for buckling is then that

$$T_i \geqq U_i. \tag{4}$$

According to Rayleigh's Principle [20], the energies $U_i$ and $W_i$ calculated using deflection fields which satisfy only the boundary conditions at the edges of the plate will yield a possible solution to the buckling problem if Eq. (4) is satisfied. The solution obtained will be the correct one if and only if the deflection field also satisfies the equilibrium equation for the true buckled shape. Otherwise the solution obtained will be merely an upper bound.

The equation for the average external energy of the transverse force is, approximately,

$$T_{T_i} = -\frac{1}{4} \int\limits_0^a \int\limits_{-b_{i/2}}^{b_{i/2}} N_{y_i} \left(\frac{\partial w_i}{\partial y}\right)^2 dx\, dy. \tag{5}$$

Substituting the deflection function, $w_i$ for mode $n$ given by Eq. (1e), and the transverse force, $N_{y_i}$ for a different mode $m$ given by Eq. (1b), into Eq. (5) yields [26]:

$$T_{T_i} = -\frac{1}{64} \sum_{m=1,3,\ldots} \sum_{n=1,3,\ldots} \left[\frac{4a}{m\pi} + \frac{4am}{(4n^2-m^2)\pi}\right] (Q_{1i} \sinh \beta_{m+n} + Q_{2i} \sinh \alpha_m$$

$$+ Q_{3i} \sinh \beta_{m-n} + Q_{4i} \cosh \beta_{m+n} + Q_{5i} \cosh \alpha_m + Q_{6i} \cosh \beta_{m-n}). \tag{6}$$

In the above equation,

$$\frac{Q_{1i}}{Q_{3i}} = \frac{b_i}{4\beta_{m\pm n}}\left[-\frac{b_i}{2\beta_{m\pm n}}\left\{R_i'\frac{2n\pi}{a}\left[2A_{1i}A_{3i} - \frac{n\pi}{a}(A_{3i}A_{18i}+A_{1i}A_{17i})\right]\right.\right.$$

$$\pm S_i A_{8i}\frac{2n\pi}{a}\left[A_{1i}\left(A_{1i}-\frac{n\pi}{a}A_{18i}\right) + A_{3i}\left(A_{3i}-\frac{n\pi}{a}A_{17i}\right)\right]$$

$$+ S_i A_{5i}\frac{m\pi}{a}\left(A_{3i}-\frac{n\pi}{a}A_{17i}\right)^2 \pm 2 S_i'\frac{m\pi}{a}\left(A_{1i}-\frac{n\pi}{a}A_{18i}\right)\left(A_{3i}-\frac{n\pi}{a}A_{17i}\right)\right\}$$

$$+ b_i^2\left(\frac{1}{4} + \frac{1}{2\beta_{m\pm n}^2}\right)\left\{-\frac{3b_i}{2\beta_{m\pm n}}\left[S_i\frac{mn^2\pi^3}{a^3}A_{5i}(A_{1i}^2+A_{3i}^2)\right.\right.$$

$$\pm 2 S_i'\frac{mn^2\pi^3}{a^3}A_{1i}A_{3i}\right] + S_i A_{8i}\frac{n^2\pi^2}{a^2}(A_{1i}^2+A_{3i}^2)$$

$$+ S_i'\frac{2mn\pi^2}{a^2}\left[2A_{1i}A_{3i} - \frac{n\pi}{a}(A_{1i}A_{17i}+A_{3i}A_{18i})\right]$$

$$\pm 2 R_i'\frac{n^2\pi^2}{a^2}A_{1i}A_{3i} \pm 2 S_i A_{5i}\frac{mn\pi^2}{a^2}\left[A_{1i}\left(A_{1i}-\frac{n\pi}{a}A_{18i}\right)\right.$$

$$+ A_{3i}\left(A_{3i}-\frac{n\pi}{a}A_{17i}\right)\right]\right\} + S_i A_{8i}\left[\left(A_{1i}-\frac{n\pi}{a}A_{18i}\right)^2\right.$$

$$+ \left(A_{3i}-\frac{n\pi}{a}A_{17i}\right)^2\right] \pm 2 R_i'\left(A_{3i}-\frac{n\pi}{a}A_{17i}\right)\left(A_{1i}-\frac{n\pi}{a}A_{18i}\right)\right];$$

$$Q_{2i} = \frac{b_i}{2\,\alpha_m}\left\{\frac{b_i}{2\,\alpha_m}\left[R'_i\frac{2\,n^2\,\pi^2}{a^2}(A_{1i}A_{17i} - A_{3i}A_{18i}) - S_i\,A_{5i}\frac{m\,\pi}{a}\left(A_{3i} - \frac{n\,\pi}{a}A_{17i}\right)^2\right]\right.$$

$$+ S_i\,A_{8i}\left[\left(A_{3i} - \frac{n\,\pi}{a}A_{17i}\right)^2 - \left(A_{1i} - \frac{n\,\pi}{a}A_{18i}\right)^2\right]$$

$$+ b_i^2\left(\frac{1}{4} + \frac{1}{2\,\alpha_m^2}\right)\left[\left(\frac{3\,b_i}{2\,\alpha_m}S_i\,A_{5i}\frac{m\,n^2\,\pi^3}{a^3} - S_i\,A_{8i}\frac{n^2\,\pi^2}{a^2}\right)(A_{3i}^2 - A_{1i}^2)\right.$$

$$\left.\left. + S'_i\frac{2\,m\,n^2\,\pi^3}{a^3}(A_{3i}A_{18i} - A_{1i}A_{17i})\right]\right\};$$

$$\frac{Q_{4i}}{Q_{6i}} = \frac{b_i^2}{4\,\beta_{m\pm n}}\left[\frac{1}{2}\left\{R'_i\frac{2\,n\,\pi}{a}\left[2\,A_{1i}A_{3i} - \frac{n\,\pi}{a}(A_{3i}A_{18i} + A_{1i}A_{17i})\right]\right.\right.$$

$$\pm 2\,S_i\,A_{8i}\frac{n\,\pi}{a}\left[A_{1i}\left(A_{1i} - \frac{n\,\pi}{a}A_{18i}\right) + A_{3i}\left(A_{3i} - \frac{n\,\pi}{a}A_{17i}\right)\right]$$

$$+ S_i\,A_{5i}\frac{m\,\pi}{a}\left(A_{3i} - \frac{n\,\pi}{a}A_{17i}\right)^2 \pm 2\,S'_i\frac{m\,\pi}{a}\left(A_{1i} - \frac{n\,\pi}{a}A_{18i}\right)\left(A_{3i} - \frac{n\,\pi}{a}A_{17i}\right)\bigg\}$$

$$- \frac{b_i}{2\,\beta_{m\pm n}}\left\{S_i\,A_{8i}\frac{n^2\,\pi^2}{a^2}(A_{1i}^2 + A_{3i}^2)\right.$$

$$+ S'_i\frac{2\,m\,n\,\pi^2}{a^2}\left[2\,A_{1i}A_{3i} - \frac{n\,\pi}{a}(A_{1i}A_{17i} + A_{3i}A_{18i})\right] \pm 2\,R'_i\frac{n^2\,\pi^2}{a^2}A_{1i}A_{3i}$$

$$\pm 2\,S_i\,A_{5i}\frac{m\,n\,\pi^2}{a^2}\left[A_{1i}\left(A_{1i} - \frac{n\,\pi}{a}A_{18i}\right) + A_{3i}\left(A_{3i} - \frac{n\,\pi}{a}A_{17i}\right)\right]\bigg\}$$

$$\left.\left. + b_i^2\left(\frac{1}{8} + \frac{3}{4\,\beta_{m\pm n}^2}\right)\left[S_i\frac{m\,n^2\,\pi^3}{a^3}A_{5i}(A_{1i}^2 + A_{3i}^2) \pm 2\,S'_i\frac{m\,n^2\,\pi^3}{a^3}A_{1i}A_{3i}\right]\right]\right];$$

$$Q_{5i} = \frac{b_i^2}{4\,\alpha_m}\left\{R'_i\frac{2\,n^2\,\pi^2}{a^2}(A_{3i}A_{18i} - A_{1i}A_{17i}) + S_i\,A_{5i}\frac{m\,\pi}{a}\left(A_{3i} - \frac{n\,\pi}{a}A_{17i}\right)^2\right.$$

$$+ \frac{b_i}{\alpha_m}\left[S_i\,A_{8i}\frac{n^2\,\pi^2}{a^2}(A_{3i}^2 - A_{1i}^2) + S'_i\frac{2\,m\,n^2\,\pi^3}{a^3}(A_{1i}A_{17i} - A_{3i}A_{18i})\right]$$

$$\left. + 2\,b_i^2\left(\frac{1}{8} + \frac{3}{4\,\alpha_m^2}\right)S_i\,A_{5i}\frac{m\,n^2\,\pi^3}{a^3}(A_{1i}^2 - A_{3i}^2)\right\};$$

where,

$$\beta_{m\pm n} = \frac{(m \pm 2\,n)\,\pi\,b_i}{2\,a},$$

$$R_i = \frac{8\,a\,p_{ti}}{m^2\,\pi^2\left(\alpha_m\operatorname{csch}\alpha_m + \frac{3-\nu_i}{1+\nu_i}\cosh\alpha_m\right)},$$

$$S_i = \frac{E_i\,h_i\,m\,\pi}{2\,a\,(1+\nu_i)},$$

$$R'_i = -R_i\left(\alpha_m\coth\alpha_m + \frac{2}{1+\nu_i}\right) + S_i\,A_{6i},$$

$$S'_i = R_i + S_i\,A_{7i}.$$

The total external energy is obtained by summing Eq. (6) over as many modes $m$ and $n$ as desired. Note that the coefficients $A_{1i}$, $A_{3i}$, $A_{17i}$, $A_{18i}$ are determined for mode $n$ and $A_{5i}$, $A_{6i}$, $A_{7i}$, $A_{8i}$ are determined for mode $m$.

The equation for the internal strain energy of bending, $U_{T_i}$ using linear, small deflection theory is:

$$U_{T_i} = \frac{1}{2} D_i \int\limits_0^a \int\limits_{-b_{i/2}}^{b_{i/2}} \left\{ \left( \frac{\partial^2 w_i}{\partial x^2} + \frac{\partial^2 w_i}{\partial y^2} \right)^2 - 2(1-\nu_i) \left[ \left( \frac{\partial^2 w_i}{\partial x^2} \right) \left( \frac{\partial^2 w_i}{\partial y^2} \right) - \left( \frac{\partial^2 w_i}{\partial x \, \partial y} \right)^2 \right] \right\} dx \, dy .$$

(7)

Substituting the deflection function, $w_i$ for mode $m$ into Eq. (7) gives [26]:

$$U_{T_i} = \frac{\pi^4 D_i}{8 a^3} \sum_{m=1, 3, \ldots} m^4 (Q_{7i} + Q_{8i} \sinh 2\alpha_m + Q_{9i} \sinh^2 \alpha_m + Q_{10i} \cosh 2\alpha_m ).$$

(8)

In the above,

$$Q_{7i} = \frac{a^2 b_i}{2 m^2 \pi^2} [A_{1i}^2 (3-\nu_i) + A_{3i}^2 (1-\nu_i)] + \frac{a b_i}{m \pi} (\nu_i - 1) (A_{1i} A_{18i} + A_{3i} A_{17i});$$

$$Q_{8i} = \frac{a^3}{m^3 \pi^3} (A_{1i}^2 + A_{3i}^2) + (1-\nu_i) \frac{a}{m \pi} \left[ A_{18i} \left( A_{18i} - \frac{a}{m \pi} A_{1i} \right) \right.$$
$$\left. + A_{17i} \left( A_{17i} - \frac{a}{m \pi} A_{3i} \right) + \frac{b_i^2}{4} (A_{1i}^2 + A_{3i}^2) \right];$$

$$Q_{9i} = (1-\nu_i) \frac{2 a b_i}{m \pi} \left[ \frac{a}{m \pi} (A_{1i}^2 + A_{3i}^2) - A_{1i} A_{18i} - A_{3i} A_{17i} \right];$$

$$Q_{10i} = -(1-\nu_i) \frac{a^2 b_i^2}{2 m^2 \pi^2} (A_{1i}^2 + A_{3i}^2).$$

In the derivation of Eq. (6), the cross terms involving $\left( \frac{\partial w_i}{\partial y} \right)_m \left( \frac{\partial w_i}{\partial y} \right)_n$ with $m \neq n$ were omitted. The subscripts $m$ and $n$ indicate the $m$th and $n$th Fourier terms. Numerical results have indicated that this is justified as the series for $w_i$ converges very rapidly compared to the series for $N_{y_i}$. It was felt that the approximation involved in the method did not justify a further refinement in the external energy Eq. (6). For the internal energy, the cross terms have no effect.

In order to perform the numerical operations necessary in the analysis a computer program was written in FORTRAN IV for the IBM 7040 computer. This program was subsequently modified to run on the IBM 360-40 computer with FORTRAN IV level E. This program also includes an option whereby only a stress analysis is made. The data to be read into the program consists of:

1. Number of plates, maximum mode of the trigonometric series.
2. Boundary conditions at outside edges (either fixed or free).
3. Number of points where final stresses are to be calculated.
4. Controls for the type of output desired (i. e. stress results or buckling results).

5. Initial length, overall depth, incremental change in length.
6. $h_i$, $b_i$, $E_i$, $\nu_i$, inclination and unit weight for each plate.
7. Initial uniform load on horizontal projection, load increment, maximum load.

Briefly, the program carries out a stress analysis for some load level using the method outlined by GOLDBERG and LEVE [9], calculates $A_{1i}$ through $A_{18i}$, $T_{T_i}$ and $U_{T_i}$ for each plate and stores the energy values. The load is then incremented and the process repeated which results in new values for $T_{T_i}$ and $U_{T_i}$. The differences between old and new values of $T_{T_i}$ and $U_{T_i}$ are calculated and thus values of $T_i$ and $U_i$ for each plate are obtained. Eq. (4) is tested for each plate and if it is not satisfied the load is once again incremented and new energy differences are obtained. This process continues until Eq. (4) is satisfied for some plate at which time the non-dimensionalized buckling load $(q_{cr}/E)$ is printed out. The entire analysis is then repeated for as many structure lengths as desired which finally yields a curve of buckling load versus length to depth ratio.

## Shear-Longitudinal Buckling Analysis

The effect of in-plane shearing and longitudinal stresses on the buckling of a plate element is based upon the work of LUNDQUIST and STOWELL [12, 17, 18]. The following approximations are employed in applying the previously developed plate buckling equations to the folded plate element.

1. The element is divided longitudinally into strips. Each strip is assumed to be simply supported along its transverse edges and to be elastically supported with regard to rotation along its longitudinal edges. The deflections, $w_i$, along the longitudinal edges are assumed to be zero (see Fig. 2).
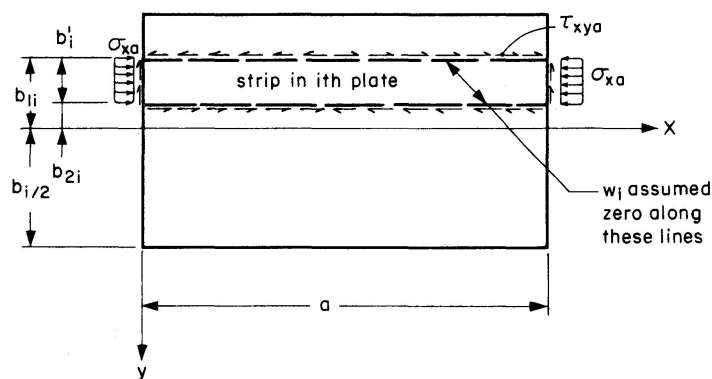


Fig. 2. Strip element of typical ($i$th) plate.

2. Each strip is assumed to be acted upon by constant shearing and longitudinal stresses obtained by averaging the actual stresses over its width and length.

3. The rotational stiffness along an edge, $S_0$, is defined by the equation,

$$S_0 = \frac{M_y}{4\theta} \tag{9}$$

for each mode and $M_y$ and $\theta$ are given by Eqs. (1a) and (1f).

4. With regard to shear buckling, the length to width ratio of the strip is assumed to be infinite.

5. The critical shearing and longitudinal stresses are [12, 18]:

$$\tau_{xy_{cr}} = \frac{\pi^2 E_i h_i^2}{12(1-\nu_i^2) b_i'^2} k_s, \tag{10}$$

$$\sigma_{x_{cr}} = \frac{\pi^2 E_i h_i^2}{12(1-\nu_i^2) b_i'^2} k_c, \tag{11}$$

in which $k_s$ and $k_c$ are the shear buckling and longitudinal buckling coefficients which depend upon the stiffness of the restraining medium. These are set forth in the Appendix.

6. The interaction of shear buckling and longitudinal buckling is assumed to be given with sufficient accuracy by the following formula [17, 19]:

$$\left(\frac{\tau_{xy_a}}{\tau_{xy_{cr}}}\right)^2 + \frac{\sigma_{x_a}}{\sigma_{x_{cr}}} \geqq 1, \tag{12}$$

in which $\tau_{xy_a}$ and $\sigma_{x_a}$ are respectively the average shearing and average longitudinal stress in a strip.

The average shearing stress for a strip $\tau_{xy_a}$ is determined by integrating the shearing stress $\tau_{xy}$ over the half length and width of the strip and dividing by the half area, or,

$$\tau_{xy_a} = \frac{2}{a b_i'} \int_0^{a/2} \int_{b_{1i}}^{b_{2i}} \sum_{m=1,3,\ldots} \frac{N_{xy}}{h_i} dx\, dy. \tag{13}$$

$N_{xy}$ is expressed by Eq. (1d) for a given mode $m$ of the trigonometric series. Substituting this function in Eq. (13) yields:

$$\tau_{xy_a} = \frac{2}{b_i' \pi} \sum_{m=1,3,\ldots} \frac{(-1)^{\frac{m+3}{2}}}{m} \left( Q_{11i} \cosh\frac{m\pi b_{2i}}{a} + Q_{12i} \cosh\frac{m\pi b_{1i}}{a} \right.$$
$$\left. + Q_{13i} \sinh\frac{m\pi b_{2i}}{a} + Q_{14i} \sinh\frac{m\pi b_{1i}}{a} + C_{pi} \right), \tag{14}$$

where      $Q_{11i} = b_{2i}(2 C_{pi}\lambda_{6m} + D_m' A_{13i}) + \frac{a}{m\pi} D_m'(A_{14i} - A_{15i});$

$$Q_{12i} = -b_{1i}(2 C_{pi}\lambda_{6m} + D_m' A_{13i}) - \frac{a}{m\pi} D_m'(A_{14i} - A_{15i});$$

$$Q_{13i} = -2 C_{pi} \lambda_{6m} \frac{a}{m\pi} \left( 1 + \alpha_m \coth \alpha_m + \frac{1-\nu_i}{1+\nu_i} \right)$$

$$+ D'_m \left( -\frac{a}{m\pi} A_{13i} + A_{15i} b_{2i} + \frac{a}{m\pi} A_{16i} \right);$$

$$Q_{14i} = 2 C_{pi} \lambda_{6m} \frac{a}{m\pi} \left( 1 + \alpha_m \coth \alpha_m + \frac{1-\nu_i}{1+\nu_i} \right)$$

$$+ D'_m \left( \frac{a}{m\pi} A_{13i} - A_{15i} b_{1i} - \frac{a}{m\pi} A_{16i} \right);$$

$$C_{pi} = \frac{4 a \, p_{ti}}{h_i \, m^2 \, \pi^2};$$

$$D'_m = \frac{E_i \, m \, \pi}{2 \, (1 + \nu_i) \, a}.$$

$b_{1i}$ and $b_{2i}$ correspond to values of $y$ at edges 1 and 2 of a strip and $b'_i$ is the strip width.

The average longitudinal stress $\sigma_{x_a}$ for a strip is determined by integrating the longitudinal stress over the length and width of the strip and dividing by the strip area as:

$$\sigma_{x_a} = \frac{1}{a \, b'_i} \int_0^a \int_{b_{1i}}^{b_{2i}} \sum_{m=1,3,\ldots} \sigma_x \, dx \, dy = \frac{1}{\pi} \sum_{m=1,3,\ldots} \frac{1}{m} (\bar{\sigma}_{x_1 i} + \bar{\sigma}_{x_2 i}), \qquad (15)$$

where $\bar{\sigma}_{x_1 i}$, $\bar{\sigma}_{x_2 i}$ are the maximum longitudinal stresses for mode $m$ at edges 1 and 2 of the strip respectively. This expression is obtained using a linear distribution of $\sigma_x$ in the $y$ direction which is a valid approximation even for the smallest length to depth ratio (approximately five to one) considered in this work.

The values of $\bar{\sigma}_{x_1 i}$, $\bar{\sigma}_{x_2 i}$ are determined from Eq. (1c) by substituting for $y$ the values of $b_{1i}$ and $b_{2i}$, for $x$ the value $a/2$, and by dividing by $h_i$.

A computer program was written in FORTRAN IV level E for the IBM 360-40 computer to perform the necessary calculations in this analysis. The following data is needed for the program:

1. Number of plates, maximum mode of the trigonometric series.
2. Boundary conditions at outside edges.
3. Controls for desired output.
4. Maximum number of strips for calculation of critical stresses in the half width of each plate.
5. Initial length, overall depth, incremental change in length.
6. $h_i$, $b_i$, $E_i$, $\nu_i$, inclination and unit weight for each plate.
7. Initial uniform load on horizontal projection, load increment, maximum load.

For a given load and strip width the stresses throughout the structure and the coefficients $A_{1i}$ through $A_{18i}$ for each plate are determined. For each strip in the structure the edge stiffnesses and the minimum average shear and longitudinal buckling coefficients as given by LUNDQUIST and STOWELL [12, 17, 18] are calculated. The values of $\tau_{xy_a}$ and $\sigma_{x_a}$ obtained from Eqs. (14) and (15) for each strip are determined and the interaction equation, Eq. (12), is applied. If the equation is not satisfied for any strip, the load is increased and the entire procedure is repeated. When Eq. (12) is satisfied for some strip the value of the buckling load $(q_{cr}/E)$ is stored and the process is repeated for a new strip width. The new value of the buckling load obtained is compared to the previous value and the smaller is retained. When the minimum buckling value is determined the process is terminated.

The above analysis is repeated for different structure lengths to obtain a curve of $\frac{q_{cr}}{E}$ $vs$ $\frac{a}{d}$.

## Results of Buckling Analyses

Five examples of folded plate roofs were analyzed using the above procedures. These are shown in Figs. 3 and 4. Fig. 3 shows the cross-sections of two full scale concrete roofs. Fig. 4 shows the cross-sections for three types of small scale, aluminum model folded plate roofs.

Dimensionless critical load versus span to depth ratio curves for these structures obtained from the computer programs described previously are presented in Figs. 5 through 9. The curves for transverse buckling were obtained using three modes of the trigonometric series. The load tolerance was $\pm 2.5$ psf. In each case the theory indicated that the inclined plates buckled first. The computer running time was approximately one hour for each curve.

The curves for shear-longitudinal buckling were obtained using three modes of the trigonometric series and a load tolerance of $\pm 5$ psf. The computer running time for each curve was approximately two hours. The Type I roofs exhibited buckling in the top plate due primarily to the longitudinal stresses. In the Type II roofs the inclined plates buckled under the combination of shearing
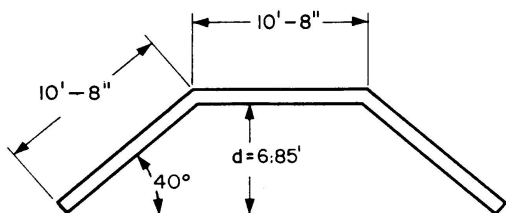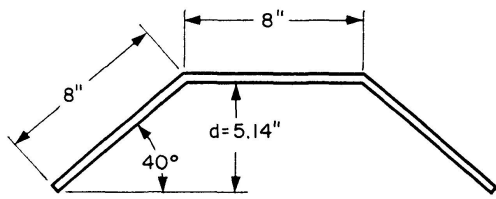


$h = 1.97''$, $\nu = 0.2$. Unit weight $= 150$ lb/ft³.

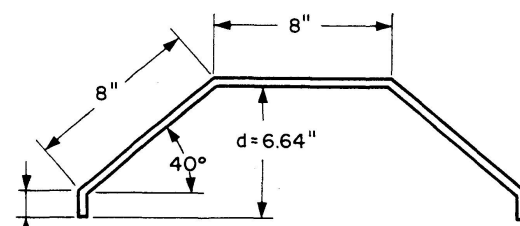Fig. 3 a. Concrete roof, type I cross-section.
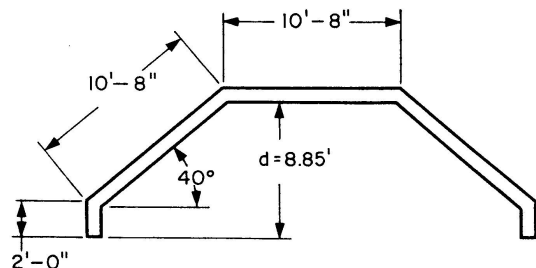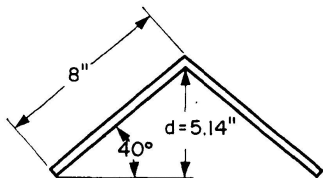
$h = 1.97''$, $\nu = 0.2$. Unit weight $= 150$ lb/ft³.

Fig. 3 b. Concrete roof, type II cross-section.

Type I cross-section

Type II cross-section

Type III cross-section

$h = 0.0625''$, $v = 1/3$. Unit weight $= 170.5$ lb/ft$^3$.

Fig. 4. Aluminum model roofs.

and longitudinal stresses for span to depth ratios less than about eight to one. For larger ratios the center plates buckled under the action of longitudinal stresses. The Type III roofs buckled under a combination of shearing and longitudinal stresses. The optimum number of strips for inclined plate buckling was two and for the center plate buckling was one.

From Figs. 5 through 9 comparisons between the transverse and shear-longitudinal critical load curves indicate that transverse buckling predominates



A – "transverse buckling"
B – "shear–longitudinal buckling"

Fig. 5. Critical load versus span to depth ratio for type I concrete roof.
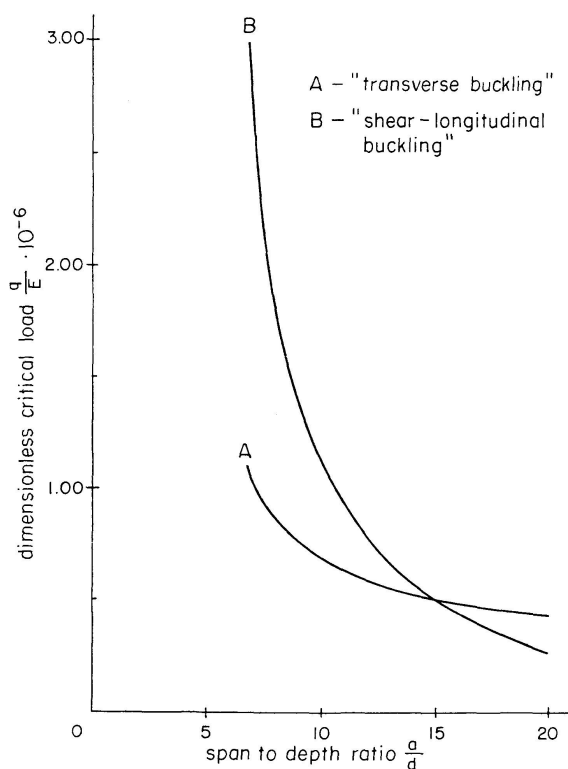


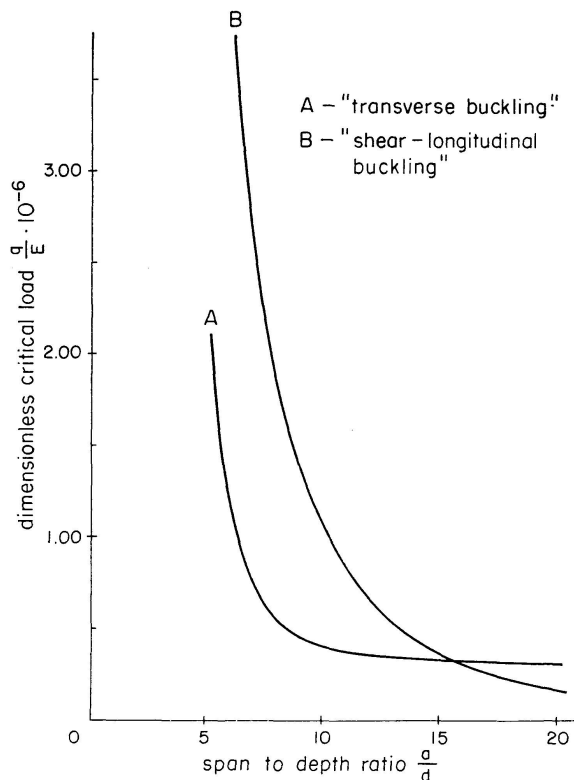A – "transverse buckling"
B – "shear–longitudinal buckling"

Fig. 6. Critical load versus span to depth ratio for type II concrete roof.
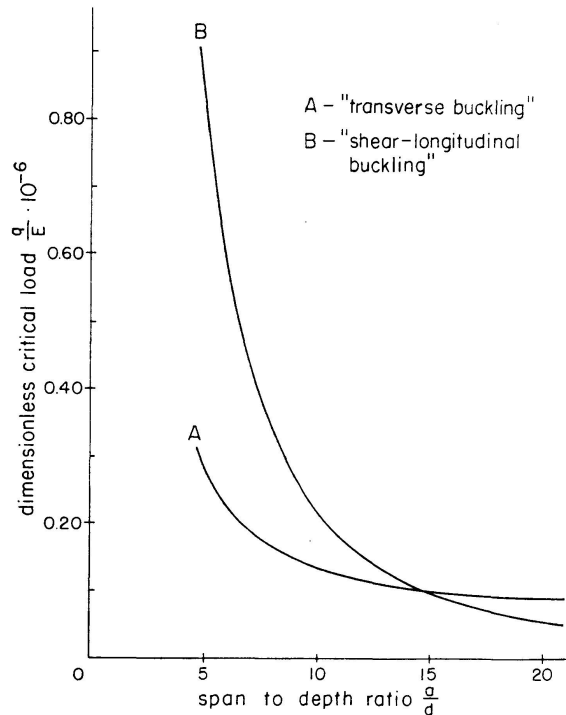
Fig. 7. Critical load versus span to depth
ratio for type I aluminum model roof.
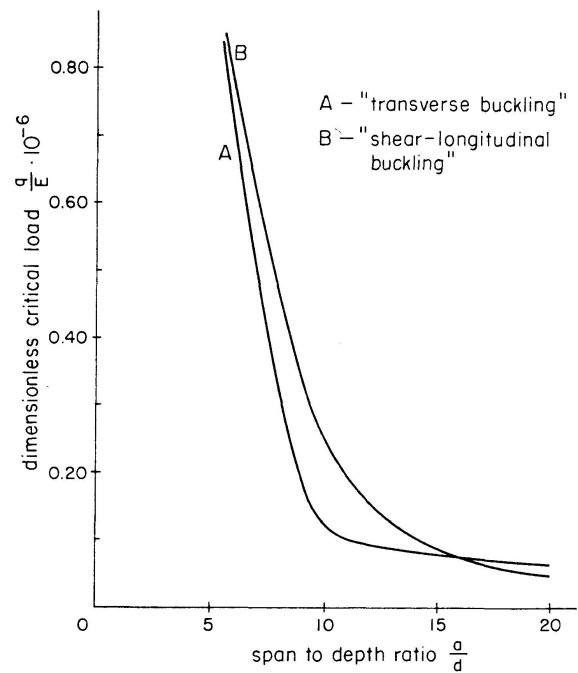


Fig. 8. Critical load versus span to depth
ratio for type II aluminum model roof.

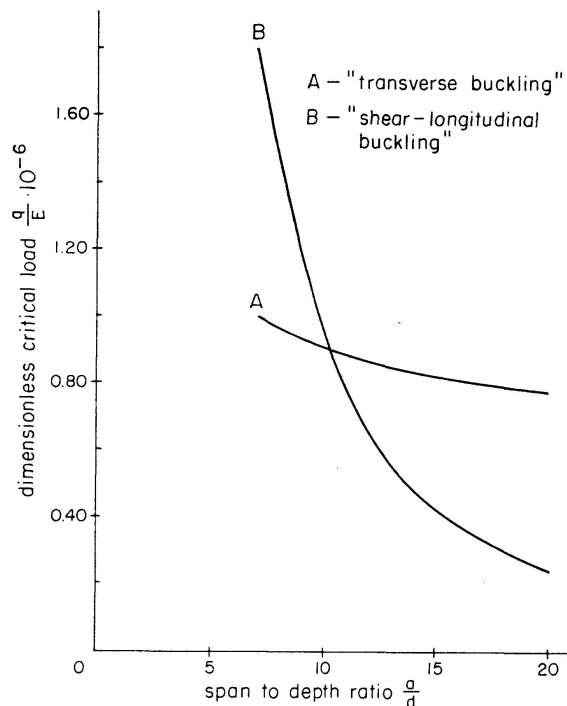

Fig. 9. Critical load versus span to depth
ratio for type III aluminum model roof.

for span to depth ratios less than about fifteen to one for Type I and II struc-
tures and ten to one for Type III structures.

As is to be expected, the results indicate that folded plate structures with
small span to depth ratios have very high buckling loads; but as the span to

depth ratio increases the buckling load decreases rapidly. Beyond a span to depth ratio of approximately ten to one the transverse buckling curves decrease very slowly whereas the shear-longitudinal curves decrease at a higher rate.

## Conclusions

An analysis of folded plate structures to predict loads at which its plate elements will buckle has been presented. This problem was treated by introducing the approximation that one of two types of stress patterns would create the buckled state; that is, either transverse in-plane stresses would cause buckling or else a combination of shearing and longitudinal in-plane stresses would. In reality, all of these stresses acting together will cause buckling.

The energy method employed in the transverse buckling analysis will always lead to an upper bound estimate of the critical load. In applying this method, the effect of the surface loads was essentially neglected. As reported by BLEICH [3], the surface load on a plate may increase or decrease the buckling strength depending upon the deflection pattern in the buckled state and the end conditions.

The shear-longitudinal buckling analysis presented herein utilizes the work of others. The formulas for critical shearing stress, critical longitudinal stress, and the interaction between the two are based upon the energy principle and upon the assumption that constant stresses pertain throughout the region of interest. This results in a prediction of constant length between the nodal points of the buckled surface. In the actual case, the stresses vary in a non-linear fashion along the length of the structure but were, for purposes of simplification, assumed to be constant throughout each plate. This approximation has been used previously in treating the problem of local buckling of beam flanges and webs [3].

In summary, the following conclusions may be drawn from this study:

1. Folded plate structures of practical dimensions, subjected to uniformly distributed, surface loads, may, in some instances, exhibit local plate buckling.

2. As a consequence of the above statement, it appears likely that present design methods for folded plates which do not take into account the possibility of buckling may be unconservative.

3. The type of local buckling which predominates depends upon the span to depth ratio and the geometric properties of the cross-section. Results obtained in this study indicate that buckling will be caused mainly by transverse stresses for small span to depth ratios and by shearing and longitudinal stresses for large span to depth ratios.

4. There are many parameters that affect the buckling strength which should be considered in addition to those used in this study. Among these are

plate thickness, plate inclination, shape of cross-section, presence of intermediate stiffeners, multiple-cell cross-sections and type of surface load. Some of these topics will be considered in subsequent reports.

## Acknowledgements

## Appendix I. Notation

$A_{1i}$—$A_{18i}$ = Force-displacement coefficients for $i$th plate.

$D_i$ = $\dfrac{E_i h_i^3}{12\left(1-v_i^2\right)}$.

$D_{1i}$ = $\dfrac{E_i h_i^3}{24\left(1+v_i\right)}$.

$D_{2i}$ = $\dfrac{E_i h_i}{2\left(1+v_i\right)}$.

$D_m'$ = $\dfrac{E_i m \pi}{2\left(1+v_i\right)a}$.

$E_i, v_i$ = Young's Modulus and Poisson's Ratio respectively for the $i$th plate.

$M_{x_i}, M_{y_i}, M_{xy_i},$
$N_{x_i}, N_{y_i}, N_{xy_i},$ = Internal moments, forces, shears in the $i$th plate.
$Q_{x_i}, Q_{y_i}$

$M_{Fy_i}, N_{Fx_i}, N_{Fy_i},$ = Internal moment, forces, shears in the $i$th plate corre-
$N_{Fxy_i}$   sponding to fixity at the ridges.

$Q_{1i}$—$Q_{14i}$ = Coefficients in external energy equation, internal energy equation and average shear equation.

$R_i, R_i', S_i, S_i', C_{pi}$ = Coefficients in expressions for $Q_{1i}$—$Q_{14i}$.

$U_i, T_i$ = Change in internal strain energy and external energy of transverse forces respectively in $i$th plate.

$a$ = Length of structure.

$b_i$ = Width of $i$th plate.

$b_i', b_{1i}, b_{2i}$ = Width and edges of longitudinal strip in $i$th plate respectively.

$d$ = Depth of roof cross-section.

$h_i$ = Thickness of $i$th plate.

$j, k$ = The edges of the $i$th plate corresponding to $y = \frac{1}{2} b_i$ and $y = -\frac{1}{2} b_i$ respectively.

$k_c$ = Plate longitudinal stress buckling coefficient.

$$= \frac{\left[\frac{\pi^2}{120}\left(\frac{b_i'}{\lambda}\right)^2 + \frac{1}{6} + \left(\frac{\lambda}{b_i'}\right)^2\right]\epsilon^2 + \left(1 + \frac{\epsilon}{2}\right)\left(\frac{b_i'}{\lambda} + \frac{\lambda}{b_i'}\right)^2 \left[\frac{1}{2}\left(1 + \frac{\epsilon}{2}\right) - \frac{4\epsilon}{\pi^2}\right] + \frac{2\epsilon}{\pi^2}\left(\frac{\lambda}{b_i'}\right)^2}{\frac{\pi^2 \epsilon^2}{120} - \frac{4\epsilon}{\pi^2}\left(1 + \frac{\epsilon}{2}\right) + \frac{1}{2}\left(1 + \frac{\epsilon}{2}\right)^2}.$$

In the above,

$$\epsilon = \frac{4 S_0 b_i'}{D_i},$$

$\lambda$ = half wave length of assumed buckled surface,

$$S_0 = \frac{M_y}{4 \theta}.$$

$k_s$ = Plate shearing stress buckling coefficient.

$$= \frac{1}{\sin 2\varphi}\left[\left(\frac{b_i'}{\lambda}\right)^2 \frac{1}{\cos^2 \varphi} + \left(\frac{\lambda}{b_i'}\right)^2 C_1 \cos^2 \varphi + C_2 (1 + 2\sin^2 \varphi)\right].$$

In the above,

$$C_1 = \frac{\epsilon^2\left(\frac{1}{8} - \frac{1}{\pi^2}\right) + \epsilon\left(\frac{1}{2} - \frac{2}{\pi^2}\right) + \frac{1}{2}}{\epsilon^2\left(\frac{\pi^2}{120} - \frac{2}{\pi^2} + \frac{1}{8}\right) + \epsilon\left(\frac{1}{2} - \frac{4}{\pi^2}\right) + \frac{1}{2}},$$

$$C_2 = 2\frac{\epsilon^2\left(\frac{5}{24} - \frac{2}{\pi^2}\right) + \epsilon\left(\frac{1}{2} - \frac{4}{\pi^2}\right) + \frac{1}{2}}{\epsilon^2\left(\frac{\pi^2}{120} - \frac{2}{\pi^2} + \frac{1}{8}\right) + \epsilon\left(\frac{1}{2} - \frac{4}{\pi^2}\right) + \frac{1}{2}},$$

and,

$$\mathrm{Cos}\, \varphi = \sqrt{C_3 + \sqrt{C_3^2 + C_4}},$$

where

$$C_3 = \frac{\frac{3}{2} C_2 - 2\left(\frac{b_i'}{\lambda}\right)^2}{4 C_2 + C_1\left(\frac{\lambda}{b_i'}\right)^2},$$

$$C_4 = \frac{3\left(\frac{b_i'}{\lambda}\right)^2}{4 C_2 + C_1\left(\frac{\lambda}{b_i'}\right)^2}.$$

$k_{cm}$ = $\alpha_m \coth \alpha_m$.

$k_{tm}$ = $\alpha_m \tanh \alpha_m$.

$m, n$ = Trigonometric mode numbers.

$p_{ni}, p_{li}$ = Loads acting on the $i$th plate in the $z$ and $y$ directions respectively.

$q, q_{cr}$ = Uniform vertical live load and live load corresponding to buckling respectively.

$w_i, \theta_i$ = The $z$ component of displacement and the rotation in the $i$th plate respectively.

$\bar{u}_j, \bar{v}_{jk}, \bar{w}_{jk}, \bar{\theta}_j$
$\bar{u}_k, \bar{v}_{kj}, \bar{w}_{kj}, \bar{\theta}_k$ = The maximum values of the $x$, $y$, $z$ components of displacement and the rotation at edges $j$ and $k$ respectively of the $i$th plate.

$x, y, z$ = Coordinate directions in the $i$th plate.

$\alpha_m = \dfrac{m\,\pi\,b_i}{2\,a}$.

$\lambda_{1m} = (\alpha_m \operatorname{sech} \alpha_m + \sinh \alpha_m)^{-1}$.

$\lambda_{2m} = (\alpha_m \operatorname{csch} \alpha_m - \cosh \alpha_m)^{-1}$.

$\lambda_{3m} = (\alpha_m \operatorname{csch} \alpha_m + \cosh \alpha_m)^{-1}$.

$\lambda_{4m} = (\alpha_m \operatorname{sech} \alpha_m - \sinh \alpha_m)^{-1}$.

$\lambda_{5m} = (\alpha_m \operatorname{sech} \alpha_m - \mu_i \sinh \alpha_m)^{-1}$.

$\lambda_{6m} = (\alpha_m \operatorname{csch} \alpha_m + \mu_i \cosh \alpha_m)^{-1}$.

$\lambda_{7m} = (\alpha_m \operatorname{csch} \alpha_m - \mu_i \cosh \alpha_m)^{-1}$.

$\lambda_{8m} = (\alpha_m \operatorname{sech} \alpha_m + \mu_i \sinh \alpha_m)^{-1}$.

$\mu_i = \dfrac{3 - \nu_i}{1 + \nu_i}$.

$\mu_{1i} = \dfrac{2}{1 - \nu_i}$.

$\mu_{3i} = \dfrac{1 + \nu_i}{1 - \nu_i}$.

$\mu_{4i} = \dfrac{2\nu_i}{1 + \nu_i}$.

$\mu_{5i} = \dfrac{2}{1 + \nu_i}$.

$\mu_{6i} = \dfrac{1 - \nu_i}{1 + \nu_i}$.

$\mu_{7i} = \dfrac{3 + \nu_i}{1 + \nu_i}$.

$\sigma_x, \sigma_y, \tau_{xy}$ = Stress components in plate.

$\sigma_{x_{cr}}, \tau_{xy_{cr}}, \sigma_{x_a}, \tau_{xy_a}$ = Buckling longitudinal and shearing stresses and average longitudinal and shearing stresses respectively for a longitudinal strip.

## Appendix II. References

1. A.C.I. Standard Building Code Requirements for Reinforced Concrete. June 1963.
2. BEAUFAIT, F. W. and GRAY, G. A.: Experimental Analysis of Continuous Folded Plates. Journal of the Structural Division, A.S.C.E., Vol. 92, Feb. 1966.
3. BLEICH, F.: Buckling Strength of Metal Structures. McGraw-Hill Book Co., 1952.

4. BUDIANSKY, B., and HU, P. C.: The Lagrangian Multiplier Method of Finding Upper and Lower Limits to the Critical Stresses. Technical Note No. 1103, N.A.C.A., 1946.
5. BUDIANSKY, B., HU, P. C., and CONNOR, R. W.: Notes on the Lagrangian Multiplier Method. Technical Note No. 1558, N.A.C.A., 1948.
6. CRAEMER, H.: Design of Prismatic Shells. Journal of American Concrete Institute, Vol. 49, No. 6, Feb. 1953.
7. DE FRIES-SKENE, A. and SCORDELIS, A. C.: Direct Stiffness Solution for Folded Plates. Proceedings A.S.C.E., Vol. 90, Aug. 1964.
8. GAAFAR, I.: Hipped Plate Analysis, Considering Joint Displacements. Transactions, A.S.C.E., Vol. 119, 1954.
9. GOLDBERG, J. E. and LEVE, H. L.: Theory of Prismatic Folded Plate Structures. International Association of Bridge and Structural Engineers, Vol. 17, 1957.
10. GURALNICK, S. A. and SWARTZ, S. E.: Reinforcement of Folded Plates. ACI Journal Proceedings, Vol. 62, May, 1965.
11. KROLL, W. D.: Tables of Stiffness and Carry-Over Factors for Flat Rectangular Plates Under Compression. Wartime Report No. 1-398, N.A.C.A., 1943.
12. LUNDQUIST, E. E., and STOWELL, E. Z.: Critical Compressive Stresses for Flat Rectangular Plates Supported Along all Edges and Elastically Restrained Against Rotation Along the Unloaded Edges. N.A.C.A., Report No. 733.
13. SALVADORI, M. G.: Numerical Computation of Buckling Loads by Finite Differences. Transactions A.S.C.E., Vol. 116, 1951.
14. SCHUMANN, L., and BACK, G.: Strength of Rectangular Flat Plates Under Edge Compression. Technical Report No. 356, N.A.C.A., 1931.
15. SCORDELIS, A. C., CROY, E. L., and STUBBS, I. R.: Experimental and Analytical Study of a Folded Plate. Proceedings, A.S.C.E., Vol. 87, Dec. 1961.
16. SEETHARAMALU, K. and KULKARNI, M. G.: Analysis of Short Span Folded Plates. Proceedings, A.S.C.E., Vol. 90, June, 1964.
17. STOWELL, E. Z.: Buckling Stresses for Flat Plates and Sections. Transactions A.S.C.E., Vol. 117, 1952.
18. STOWELL, E. Z.: Critical Shear Stress of an Infinitely Long Flat Plate with Equal Restraints Against Rotation Along the Parallel Edges. N.A.C.A., Wartime Report No. L-476, 1943.
19. STOWELL, E. Z., and SCHWARTZ, E. B.: Critical Stress for an Infinitely Long Flat Plate with Elastically Restrained Edges Under Combined Shear and Direct Stress. Wartime Report No. L-340, N.A.C.A., 1943.
20. TEMPLE and BICKLEY: Rayleigh's Principle. Dover Publications, 1956.
21. TIMOSHENKO, S., and GERE, J.: Theory of Elastic Stability. McGraw-Hill Book Co., Inc., 1961.
22. WERFEL, A.: Die genaue Theorie der prismatischen Faltwerke und ihre praktische Anwendung. Publications, I.A.S.B.E., No. 14, 1954.
23. WINTER, G. and PEI, M.: Hipped Plate Construction. A.C.I. Journal, Vol. 43, Jan. 1947.
24. WINTER, G.: Strength of Thin Steel Compression Flanges. Transactions A.S.C.E., Vol. 112, 1947.
25. YITZHAKI, D.: The Design of Prismatic and Cylindrical Shell Roofs. Haifa Science Publishers, Haifa, 1958.
26. SWARTZ, S. E.: Buckling of Folded Plates. Thesis presented to Illinois Institute of Technology at Chicago, Illinois in 1967, in partial fulfillment of the requirements for the degree of Doctor of Philosophy.

## Summary

An approximate analysis of an arbitrary, single-cell, folded plate structure to predict the transverse load at which one or more of its individual constituent plates will buckle is presented. The problem is treated by introducing the approximation that one of two types of stress pattern may induce buckling; that is, either transverse in-plane stresses or a combination of shear and longitudinal in-plane stresses. The energy method employed in the transverse buckling analysis will always lead to an upper bound estimate of the critical load. In the shear-longitudinal buckling analysis, the equations for critical shearing stress, critical longitudinal stress, and the interaction between the two are based upon the energy principle and upon the assumption that constant stresses pertain throughout the region of interest.


## Résumé

Une analyse approximative des voiles prismatiques unicellulaires quelconques permet aux auteurs de prévoir la charge transversale à laquelle une ou plusieurs de ses plaques constituantes deviendront instables. Le problème est simplifié en supposant que le voilement peut être provoqué par les deux types de répartition des tensions suivants: soit par des tensions transversales planes, soit par une combinaison de tensions de cisaillement et de tensions longitudinales. La méthode énergétique appliquée à l'analyse du voilement transversal mènera toujours à une limite supérieure de la charge critique. Dans l'analyse du second cas (tensions de cisaillement et tensions longitudinales), le principe de l'énergie et la supposition de tensions constantes d'un bout à l'autre de la région intéressante permettent d'établir les équations pour la tension de cisaillement critique, la tension longitudinale critique et leur interaction.


## Zusammenfassung

Es wird eine Näherungslösung der Querlast, unter der ein oder mehrere Einzelscheiben ausbeulen, für ein beliebiges, einzelliges Faltwerk angegeben. Das Problem wird für die Näherung behandelt, daß eine oder zwei Spannungsformen Beulen verursachen, entweder ebene Querspannungen oder eine Verbindung von Schub- und ebenen Längsspannungen. Im ersten Fall führt die Energiemethode für Querbeulen immer zu einem oberen Wert der geschätzten Beullast. Im zweiten Fall des Schub-Längsbeulens fußen die Gleichungen für die Beulschub-, Beullängsspannung sowie das Zusammenwirken derselben auf dem Energieprinzip unter der Voraussetzung, daß die Spannungen im wirksamen Bereich konstant bleiben.